# MR Angiography in Pre-operative Evaluation for Fibula Free-flap Transfer Operation: Application, Branching Pattern Analysis and Septocutaneous Perforator Identification

**G. S. Sandhu[1,2], R. P. Rezaee[3], K. Wright[4], J. A. Jesberger[2], M. A. Griswold[1,4], and V. Gulani[1,2]**

[1]Radiology, University Hospitals of Cleveland, Case Western Reserve University, Cleveland, Ohio, United States, [2]Case Center for Imaging Research, Case Western Reserve University, Cleveland, Ohio, United States, [3]Case Center for Imaging Research, University Hospitals of Cleveland, Case Western Reserve University, Cleveland, Ohio, United States, [4]Biomedical Engineering, Case Western Reserve University, Cleveland, Ohio, United States

**Introduction:** In a fibula free-flap (FFF) transfer operation (FFFTO), a FFF harvested from the lower leg is used for tissue reconstruction at a recipient site. The presence of occlusive lesions and anatomic variations in branching pattern of the lower leg arterial tree and location and number of peroneal artery septocutaneous perforators (SCPs) necessitate preoperative evaluation of these patients [1]. Here we describe the application of magnetic resonance angiography (MRA) for preoperative evaluation in FFFTO candidates and investigate individual efficacy of bolus-chase and time-resolved MRA (bcMRA and trMRA, respectively) for branching pattern visualization and SCP localization.

**Methods:** In this IRB approved retrospective study, image analysis of 27 FFFTO candidates (mean age 61.6 yrs, range 27-88 yrs, M/F 22/5) who had bcMRA and trMRA at 3 T (Magnetom Verio, Siemens) using 0.10 and 0.05 mMol/Kg Gadobenate Dimeglumine (Multihance; Bracco Diagnostics Inc. Princeton, NJ, USA) respectively, was performed. bcMRA data were acquired using FLASH sequence (TR/TE/α 3.2/1.2/25º, voxel size 0.94×0.89×1 mm³). trMRA was performed using Time resolved imaging with stochastic trajectories (TWIST) technique (FLASH, TR/TE/α 2.5/1.0/22º, voxel size 1.54×1.25×1.5 mm³, 2.3s/ image). Maximum intensity projection (MIP) technique was used for data analysis. Data from both legs were analyzed for all patients (one patient had single leg). The branching pattern was identified and total number of SCPs and distance of their origin from the lower end of fibula were separately calculated for each leg from the two sets of MIPs and the results were combined. The branching pattern was classified into patterns described in the literature [2] and the two kinds of images were compared in terms of proper branching pattern visualization. The total number of SCPs in all legs was calculated and distribution pattern of distance of their origin from the lower end of fibula was studied. The average number of SCPs in one leg was calculated. The total number of SCPs identified from trMRA and bcMRA was also calculated.

**Results:** Various branching patterns observed in this study are shown in Figure 1. The pattern I-A, I-B, II-A, II-B III-A, III-B and III-D was observed in 42 (79.2%), 2 (3.8%), 1 (1.9%), 1 (1.9%), 4 (7.5%), 1 (1.9%), and 2 (3.8%) legs, respectively. The branching pattern was classified in all 53 legs from trMRA and was not possible from bcMRA in 2 legs. The total number of visible SCPs is 84. The average number (range) of visible SCPs in one leg is 1.58±1.05 (0-5). The SCP density is highest in the region between 10 and 30 cm from lower end of the fibula (Figure 2). A total of 82 (97.6%) and 22 SCPs (26.2%) are visible from bcMRA and trMRA, respectively.

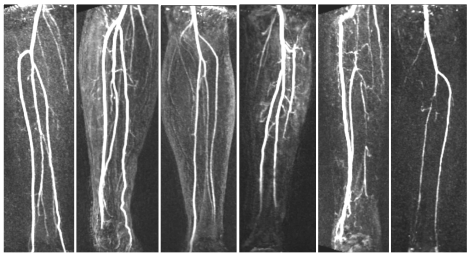

Figure 1: Various branching patterns as observed from trMRA images. Patterns I-A, I-B, II-A, III-A, III-B and III-D can be seen (left to right).

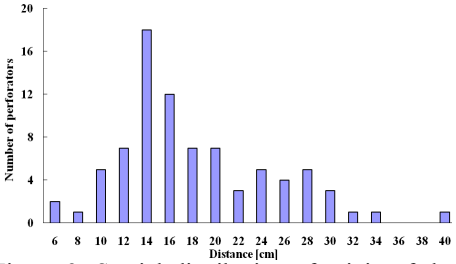


Figure 2: Spatial distribution of origin of the SCPs as function of vertical distance from lower end of the fibula.

**Discussion:** The frequency of type IA pattern and type IIIC anomaly is lower, whereas that of type IIID anomaly is higher in this study than that documented in literature [3]. In those 51 legs, in which the classification was successful from trMRA as well as bcMRA, the branching pattern types as identified from the two techniques were in agreement with each other. However, bcMRA failed to identify the branching pattern in one leg of two patients due to the presence of excessive venous contamination. The bcMRA alone would have necessitated a call-back exam in these patients. The frequency and range of the SCPs in one leg in this study matches with previous values reported from cadaver dissection [4]. However, the number of legs without a SCP in our study is relatively high likely due to low spatial resolution of the MRA techniques as compared to the SCP diameter [4]. The number of visible SCPs and the contrast between the SCPs and adjacent structures is lower in trMRA than that in bcMRA (Figures 3, 4), which likely relates to lower spatial resolution and lower Gadolinium dose employed in trMRA. The SCP visibility in particularly the trMRA can be further improved by optimizing their spatial resolution and Gadolinium contrast dose.

MRA enables the branching pattern analysis as well as SCP localization in a single step. The vascular tree can be visualized in any arbitrary plane that helps in tracing the full course of a SCP and to differentiate it from other perforator types. At our institute, the lower leg MRA of a FFFTO candidate was previously reported only in terms of the branching pattern and presence of any pathological lesion in the arterial tree. In these patients, the utility of MRA can be further enhanced by reporting the number of the SCPs and their location with respect to a fixed point in the leg, which aids in planning the location and design of the graft prior to the procedure. Pre-operative analysis may allow the surgeon to know whether or not to utilize a FFF for more complicated defects for which some surgeons may choose multiple flaps or an alternate flap such as the scapular flap, iliac crest or serratus anterior-rib flap. The use of multiple or alternative grafts lengthens the operative time and increases the post-operative morbidity. Therefore, optimum planning of the graft harvest site after comprehensive vascular analysis in patients with complicated defects will help in minimizing the patient discomfort while simplifying the surgical procedure.

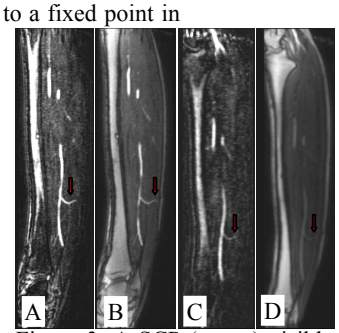


Figure 3: A SCP (arrow) visible from sagittal MIPs (3 mm thick) of subtraction and unsubtracted source data from bcMRA (A, B) and trMRA (C, D), respectively.

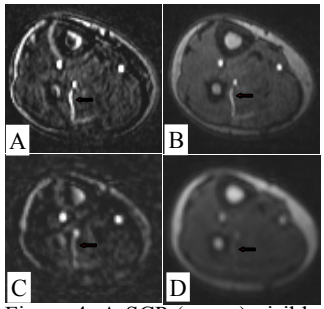


Figure 4: A SCP (arrow) visible from axial MIPs (3 mm thick) of subtraction and unsubtracted source data from bcMRA (A, B) and trMRA (C, D), respectively.

**Conclusion:** MRA images can be used to identify the lower leg arterial tree branching pattern as well as to localize the SCPs in a single step. Accurate branching pattern classification can be performed from trMRA in every leg while SCPs can be better identified from bcMRA.

**References:** 1. Fukaya E, et al. J Reconstr Microsurg 2007; 23:205-11. 2. Bardsley JL, et al. Radiology 1970; 94:581-7. 3. Kim D, et al. Ann Surg 1989; 210:776-81. 4. Yoshimura M, et al. Plast Reconstr Surg 1990; 85:917-21.

**Acknowledgments:** This work was partially supported by Siemens Medical Solutions. VG is also supported in part by NIH/NCRR 1KL2RR024990.